Leptonic and Semileptonic Charm Decays from CLEO-c

S. Stone*

Physics Department of Syracuse University
Syracuse NY, 13244, USA

I describe CLEO-c purely leptonic decay results leading to $f_{D^+} = (222.6 \pm 16.7^{+2.8}_{-3.4})$ MeV, $f_{D_s^+} = (280.1 \pm 11.6 \pm 6.0)$ MeV, and $f_{D_s^+}/f_{D^+} = 1.26 \pm 0.11 \pm 0.03$. Form-factor measurements in Cabibbo favored and suppressed pseudoscalar decays are presented. Some comparisons are made with theoretical predictions.

I. INTRODUCTION

Threshold production of $D^0\overline{D}^0$ and D^+D^- mesons at 3770 MeV, and $D_s^+D_s^{*-} + D_s^{*+}D_s^-$ mesons at 4170 MeV in e^+e^- annihilations have allowed CLEO-c to make precision measurements using purely leptonic and semileptonic charm meson decays.

II. PURELY LEPTONIC DECAYS

To extract precise information from B mixing measurements the ratio of "leptonic decay constants," f_i for B_d and B_s mesons must be well known [1]. Indeed, the recent measurement of B_s^0 mixing by CDF [2] has pointed out the urgent need for precise numbers. The f_i have been calculated theoretically. The most promising of these calculations are based on lattice-gauge theory that include the light quark loops [3]. In order to ensure that these theories can adequately predict f_{B_s}/f_{B_d} it is critical to check the analogous ratio from charm decays $f_{D_s^+}/f_{D^+}$. Here I present the most precise measurements to date of $f_{D_s^+}$, f_{D^+} [4, 5] and $f_{D_s^+}/f_{D^+}$.
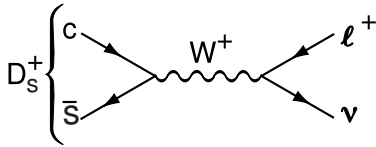

FIG. 1: The decay diagram for $D_s^+ \rightarrow \ell^+\nu$.

In the Standard Model (SM) the $D_{(s)}^+$ meson decays purely leptonically as shown in Fig. 1. The decay width is given by [6]

$$\Gamma(D_{(s)}^+ \rightarrow \ell^+\nu) = \frac{G_F^2}{8\pi} f_{D_{(s)}^+}^2 \, m_{\ell^+}^2 M_{D_{(s)}^+} \tag{1}$$
$$\times \left(1 - m_{\ell^+}^2/M_{D_{(s)}^+}^2\right)^2 |V_{cq}|^2 \ ,$$

where m_{ℓ^+} and $M_{D_{(s)}^+}$ are the ℓ^+ and $D_{(s)}^+$ masses, $|V_{cq}|$ is the CKM element appropriate to either D^+ (V_{cd}) or D_s^+ (V_{cs}) decay and G_F is the Fermi constant.

New physics can affect the expected widths; any undiscovered charged bosons would interfere with the SM W^+. These effects may be difficult to ascertain, since they would simply change the value of the f_i's. The ratio $f_{D_s^+}/f_{D^+}$, however, is much better predicted in the SM than the values individually. Akeroyd predicts that the presence of a charged Higgs boson would suppress this ratio significantly [7]. In addition, the ratio of decay rates to different leptons are fixed only by well-known masses in Eq. 1. For example, the SM prediction for $\Gamma(D_s^+ \rightarrow \tau^+\nu)/\Gamma(D_s^+ \rightarrow \mu^+\nu)$ is 9.72. In general, any deviation from a predicted ratio would be a manifestation of physics beyond the SM, and would be a clear violation of lepton universality [8].

CLEO previously measured $f_{D_s^+}$ using 4.8 fb^{-1} of continuum annihilation data at or just below the $\Upsilon(4S)$ [9]. This analysis introduced a number of new ideas: (i) The γ and μ^+ from $D_s^{*+} \rightarrow \gamma D_s^+$; $D_s^+ \rightarrow \mu^+\nu$ were detected directly, and the ν 4-vector was inferred from missing energy and momentum measurement in half of the event, where the event half was determined using the normal to the thrust axis. (ii) The ν 4-vector was corrected to get the right D_s^+ mass and $\Delta M = M(\gamma\mu^+\nu) - M(\mu^+\nu)$ was examined (see Fig. 2(a)). (ii) The background was measured using the same technique with e^+ identified instead of μ^+, relying on the large suppression of the e^+ rate compared with the μ^+ rate. (iv) The reaction $D^{*0} \rightarrow \gamma D^0$; $D^0 \rightarrow K^-\pi^+$, where the π^+ is first found and then ignored was used to evaluate efficiencies. The published result was

$$\frac{\Gamma(D_s^+ \rightarrow \mu^+\nu)}{\Gamma(D_s^+ \rightarrow \phi\pi^+)} = 0.173 \pm 0.023 \pm 0.035 \ . \tag{2}$$

BaBar recently performed an improved analysis based on these techniques [10]. They used 230 fb^{-1} of continuum data. To reduce the background and systematic errors they fully reconstruct a D^0, D^+ or D^* meson in the event with the γ and μ^+ candidate. Their data are shown in Fig. 2(b). They find

$$\frac{\Gamma(D_s^+ \rightarrow \mu^+\nu)}{\Gamma(D_s^+ \rightarrow \phi\pi^+)} = 0.143 \pm 0.018 \pm 0.006 \ . \tag{3}$$
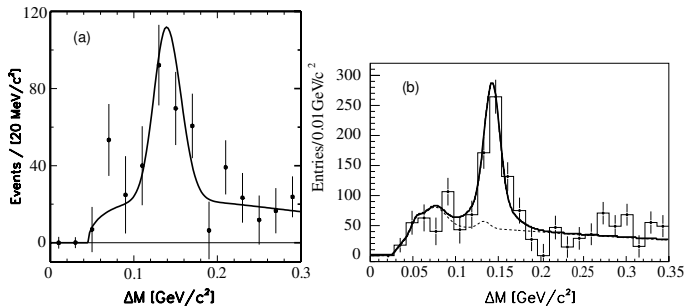
*Electronic address: stone@physics.syr.edu

FIG. 2: The ΔM distributions for μ^+ candidates after the e^+ subtraction from (a) CLEO and (b) BaBar. The solid curves are fits to signal plus background.

Both of these results, however, need to assume a value for $\mathcal{B}(D_s^+ \to \phi\pi^+)$ [11], in order to extract the decay constant. Because of interferences among the final state $K^+K^-\pi^+$ particles, the rate for $\phi\pi^+$ depends on experimental cuts [12], and thus has an inherent, sizable, systematic error. (Other experiments also normalize with respect to this or other less well known modes.)

CLEO-c eliminates this uncertainty by making absolute measurements. We tag a D_s^- decay and search for three separate decay modes of the D_s^+: (1) $\mu^+\nu$ and $\tau^+\nu$, where (2) $\tau^+ \to \pi^+\overline{\nu}$ or (3) $\tau^+ \to e^+\nu\overline{\nu}$ [13]. For the first two analyses we require the detection of the γ from the $D_s^* \to \gamma D_s$ decay, irrespective if the D_s^* is the parent of the tag or the leptonic decay. In either case, for real $D_s^* D_s$ events, the missing mass squared recoiling against the photon and the D_s^- tag should peak at $M_{D_s^+}$ and is given by

$$\text{MM}^{*2} = (E_{\text{CM}} - E_D - E_\gamma)^2 - (\overrightarrow{p}_{\text{CM}} - \overrightarrow{p}_D - \overrightarrow{p}_\gamma)^2 ,$$

where E_{CM} ($\overrightarrow{p}_{\text{CM}}$) is the center of mass energy (momentum), E_D ($\overrightarrow{p}_D$) and E_γ ($\overrightarrow{p}_\gamma$) are the energy of the fully reconstructed D_s^- tag, and the additional photon. In performing this calculation we use a kinematic fit that constrains the decay products of the D_s^- to $M_{D_s^+}$ and conserves overall momentum and energy.

The MM^{*2} from the D_s^- tag sample data is shown in Fig. 3. There are $11880\pm399\pm511$ signal events in the interval $3.978 > \text{MM}^{*2} > 3.776$ GeV^2.
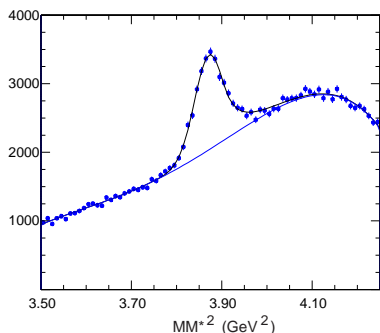

FIG. 3: The MM^{*2} distribution from events with a photon in addition to the D_s^- tag. The curve is a fit to the Crystal Ball function and a 5th order Chebychev background function.

Candidate $D_s^+ \to \mu^+\nu$ events are searched for by selecting events with only a single extra track with opposite sign of charge to the tag; we also require that there not be an extra neutral energy cluster in excess of 300 MeV. Since here we are searching for events where there is a single missing neutrino, the missing mass squared, MM^2, evaluated by taking into account the seen μ^+, D_s^-, and the γ should peak at zero, and is given by

$$\begin{aligned} \text{MM}^2 &= (E_{\text{CM}} - E_D - E_\gamma - E_\mu)^2 \quad (4) \\ &- (\overrightarrow{p}_{\text{CM}} - \overrightarrow{p}_D - \overrightarrow{p}_\gamma - \overrightarrow{p}_\mu)^2 , \end{aligned}$$

where E_μ ($\overrightarrow{p}_\mu$) is the energy (momentum) of the candidate muon track.

We also make use of a set of kinematical constraints and fit the MM^2 for each γ candidate to two hypotheses one of which is that the D_s^- tag is the daughter of a D_s^{*-} and the other that the D_s^{*+} decays into γD_s^+, with the D_s^+ subsequently decaying into $\mu^+\nu$.

The kinematical constraints are the total momentum and energy, the energy of the either the D_s^* or the D_s, the appropriate $D_s^* - D_s$ mass difference and the invariant mass of the D_s tag decay products. This gives us a total of 7 constraints. The missing neutrino four-vector needs to be determined, so we are left with a three-constraint fit. We perform a standard iterative fit minimizing χ^2. As we do not want to be subject to systematic uncertainties that depend on understanding the absolute scale of the errors, we do not make a χ^2 cut, but simply choose the photon and the decay sequence in each event with the minimum χ^2.

We consider three mutually exclusive cases: (i) the track deposits < 300 MeV in the calorimeter, characteristic of a non-interacting π^+ or a μ^+; (ii) the track deposits > 300 MeV in the calorimeter, characteristic of an interacting π^+; (iii) the track satisfies our e^+ selection criteria. The MM^2 distributions are shown in Fig. 4. The separation between μ^+ and π^+ is not unique. Case (i) contains 99% of the μ^+ but also 60% of the π^+, while case (ii) includes 1% of the μ^+ and 40% of the π^+ [5]. There is a clear peak in Fig. 4(i), due to $D_s^+ \to \mu^+\nu$. Furthermore, the events in the region between $\mu^+\nu$ peak and 0.20 GeV^2 are dominantly due to the $\tau^+\nu$, $\tau^+ \to \pi^+\overline{\nu}$ decay. The best result comes from summing case (i) and case (ii) below MM^2 of 0.20 GeV^2; higher values of MM^2 admit background from $\eta\pi^+$ and $K^0\pi^+$ final states. The branching fractions are summarized in Table I. The absence of any detected e^+ opposite to our tags allows us to set the upper limit listed in Table I.

CLEO-c also uses $D_s^+ \to \tau^+\nu$, $\tau \to e^+\nu\bar{\nu}$. Electrons of opposite sign to the tag are detected in events without any additional charged tracks, and determining the unmatched energy in the crystal calorimeter ($\text{E}_{\text{CC}}^{\text{extra}}$). This energy distribution is shown in Fig. 5. Requiring $\text{E}_{\text{CC}}^{\text{extra}} < 400$ MeV, enhances the signal. The branching ratio resulting from this analysis is also listed in Table I.

CLEO-c's published result for f_{D^+} [4] uses the "double-tag" method at 3770 GeV, where $D^+ D^-$ final states are
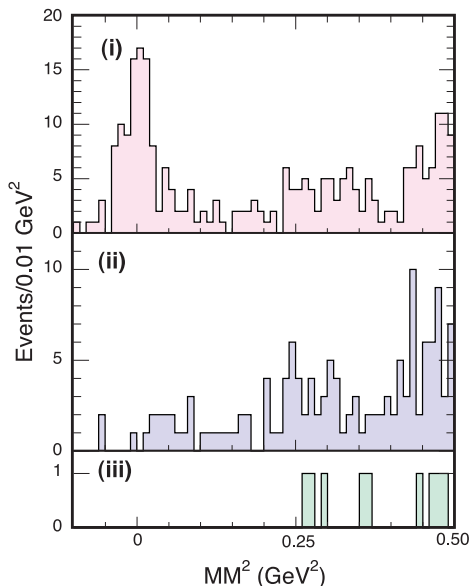
FIG. 4: The MM^2 distributions from data using D_s^- tags and one additional opposite-sign charged track and no extra energetic showers (see text).

TABLE I: Measured D_s^+ Branching Fractions

Final State	$\mathcal{B}$ (%)
$\mu^+\nu$	$0.657 \pm 0.090 \pm 0.028$
$\mu^+\nu^\dagger$	$0.664 \pm 0.076 \pm 0.028$
$\tau^+\nu$, $(\tau^+ \to \pi^+\nu)$	$7.1 \pm 1.4 \pm 0.3$
$\tau^+\nu$, $(\tau^+ \to e^+\nu\bar{\nu})$	$6.29 \pm 0.78 \pm 0.52$
$\tau^+\nu$ (average)	6.5 ± 0.8
$e^+\nu$	$< 3.1 \times 10^{-4}$ (90% cl)

$\dagger$ From summing the $\mu^+\nu$ and $\tau^+\nu$ contributions for MM^2 < 0.20 GeV^2.

produced without any extra particles. Here one D^- is fully reconstructed and then there are enough kinematic constraints to search for $D^+ \to \mu^+\nu$ by constructing the missing mass-squared (MM^2) opposite the D^- and the muon. Fifty signal events are found of which 2.8 are estimated background, resulting in:

$$\mathcal{B}(D^+ \to \mu^+\nu) = (4.40 \pm 0.66^{+0.09}_{-0.12}) \times 10^{-4} \ . \quad (5)$$

The decay constant f_{D^+} is obtained from Eq. (1) using 1.040 ± 0.007 ps as the D^+ lifetime, and $|V_{cd}| = 0.2238 \pm 0.0029$, giving

$$f_{D^+} = (222.6 \pm 16.7^{+2.8}_{-3.4}) \text{ MeV} \ . \quad (6)$$

CLEO-c also sets limits on $\mathcal{B}(D^+ \to e^+\nu_e) < 2.4 \times 10^{-5}$, [4] and $\mathcal{B}(D^+ \to \tau^+\nu)$ branching ratio to $< 2.1 \times 10^{-3}$ at 90% C.L. [14]. These limits are consistent with SM expectations.

For D_s^+ decays, we first test lepton universality in

$$R \equiv \frac{\Gamma(D_s^+ \to \tau^+\nu)}{\Gamma(D_s^+ \to \mu^+\nu)} = 9.9 \pm 1.9 \ , \quad (7)$$
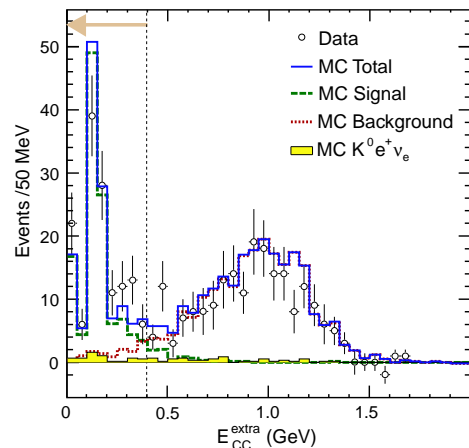

FIG. 5: The extra calorimeter energy from data (points), compared with the Monte Carlo simulated estimates of semileptonic decays in general (dotted), the $K^0e^+\nu$ mode specifically (shaded), as a sub-set of the semileptonics, and the expectation from signal (dashed). The peak near 150 MeV is due to the γ from $D_s^* \to \gamma D_s$ decay. (The sum is also shown (line).) The arrow indicates the selected signal region below 0.4 GeV.

consistent with the predicted value of 9.72. Combining our branching ratios determinations and using $\tau_{D_s^+}=0.49$ ps and $|V_{cs}|=0.9737$, we find

$$f_{D_s} = (280.1 \pm 11.6 \pm 6.0) \text{ MeV, and} \quad (8)$$
$$f_{D_s^+}/f_{D^+} = 1.26 \pm 0.11 \pm 0.03.$$

These preliminary results are consistent with most recent theoretical models. As examples, unquenched lattice [15] predicts $1.24 \pm 0.01 \pm 0.07$, while one quenched lattice calculation [16] gives $1.13 \pm 0.03 \pm 0.05$, with other groups having similar predictions [20].

III. SEMILEPTONIC DECAYS

One of the best ways to measure magnitudes of CKM elements is to use semileptonic decays since they are far simpler to understand than hadronic decays and the decay width is $\sim |V_{cq}|^2$. On the other hand, measurements using other techniques have obtained useful values for V_{cs} and V_{cd} [17], and thus semileptonic D decay measurements are a good laboratory for testing theories of QCD. For a D meson decaying into a single hadron (h), the decay rate can be written exactly in terms of the four-momentum transfer defined as:

$$q^2 = (p_D^\mu - p_h^\mu)^2 = m_D^2 + m_h^2 - 2E_h m_D \ . \quad (9)$$

For decays to pseudoscalar mesons and "virtually massless" leptons, the decay width is given by:

$$\frac{d\Gamma(D \to Pe^+\nu)}{dq^2} = \frac{|V_{cq}|^2 G_F^2 p_P^3}{24\pi^3} \left| f_+(q^2) \right| \ , \quad (10)$$

where p_P is the three-momentum of P in the D rest frame, and $f_+(q^2)$ is a "form-factor," whose normalization must be calculated theoretically, although its shape can be measured.

The shape measurements can distinguish between form-factor parameterizations. In general,

$$f_+(q^2) = \frac{f_+(0)}{(1-\alpha_p)(1-\frac{q^2}{m_{\text{pole}}^2})} + \frac{1}{\pi}\int_{(M_D+M_P)^2}^{\infty} dq'^2 \frac{Im\, f(q'^2)}{q'^2 - q^2},$$

which incorporates the possibility of a virtual of a nearby pole (first term) with fractional strength α_p. The integral term can be expressed in terms of an infinite series [18]. Typically it takes only a few terms to describe the data. An analytical parametrization

$$f_+(q^2) = \frac{f_+(0)}{(1 - q^2/m_{\text{pole}}^2)(1 - \alpha q^2/m_{\text{pole}}^2)} \qquad (11)$$

has become popular [19], though it has been criticized as being overly constraining [18]. Fits are typically done for $f_+(0)$ and either m_{pole} or α. Naively, setting α to zero gives the simple pole model where the pole mass corresponds to the first vector resonance in the D-P system, D_s^* for $D \to K e^- \nu$ and D^* for $D \to \pi e^- \nu$

CLEO-c uses two methods to analyze pseudoscalar decays. In the first method tags are fully reconstructed and events with a missing ν are inferred using the variable $U = E_{\text{miss}} - |P_{\text{miss}}|$, similar to MM^2, where "miss" here refers to the missing energy or momentum (see Fig. 6).
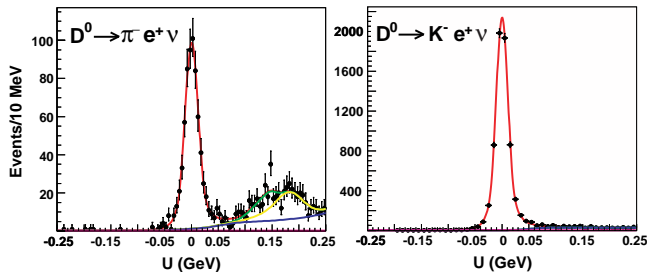

FIG. 6: U distributions using D tags in conjunction with an identified electron of opposite flavor plus a single hadron. The peak centered at zero is signal. The dashed curves indicate various backgrounds, while he solid curve shows the fit to signal plus background.

The second method consists of also using missing energy and momentum, skipping the step of reconstructing the tag, but using all of the measured charged tracks and photons. Then the D mass is reconstructed. The beam-constrained mass (M_{bc}) distributions are shown in Fig. 7.

Both cases have excellent signal to background in these modes. The ν-reconstruction has better statistical albeit poorer systematic errors. Eventually combined results will be quoted; they should not be averaged as there are a substantial number of events in common.

Form-factor shapes using the tagged sample are are shown in Fig. 8. The unquenched lattice QCD model [21] is systematically higher than our data, but not in
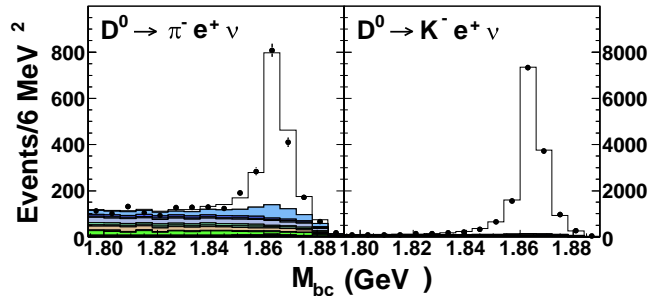

FIG. 7: M_{bc} distributions for events containing an identified electron plus a single hadron candidate. The shaded regions indicate various backgrounds.
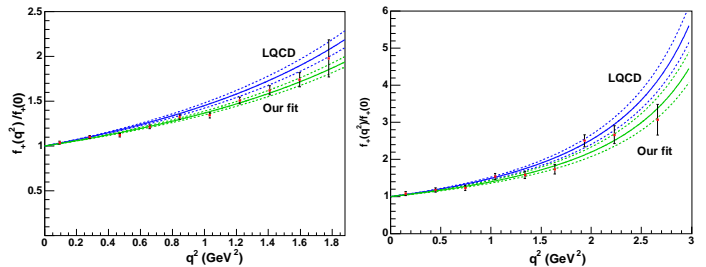

FIG. 8: CLEO-c form-factor shapes using the tagged sample. The lower curves are fits to the modified pole model, while the upper curves are fits to unquenched lattice QCD [21].

significant disagreement. Properties of these decays are listed in Table II.

Measurements of the vector decays $D \to K^* e^+ \nu$ and $\rho e^+ \nu$ can be used to determine $|V_{ub}|$ along with measurements of $B \to \rho \ell^- \bar{\nu}$ and $B \to K^* \ell^+ \ell^-$ [23]. CLEO-c has examined D vector semileptonic decays. Non-parametric form-factors in the Cabibbo favor $D^0 \to K^{*0} e^+ \nu$ decays have been measured by CLEO-c [24], following a method developed by FOCUS [25]. Cabibbo suppressed form-factors have been measured in $D \to \rho e^+ \nu$ decays. The U distribution for $\rho e^+ \nu$ decays is shown in Fig. 9. Preliminary branching fractions are listed in Table III along with observations (or limits) from other rare semileptonic decays. Selected candidates are used to measure the ratios of pole dominated form-factor ratios as $R_V = 1.40 \pm 0.25 \pm 0.03$ and $R_2 = 0.57 \pm 0.18 \pm 0.06$,

TABLE II: Properties of $D^0 \to P^- e^+ \nu$ decays (preliminary) [22]. To determine m_{pole}, α in Eq. 11 is set to zero.

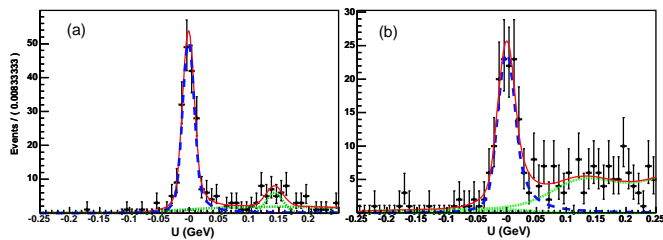| Quantity	$K^- e^+ \nu$	$\pi^- e^+ \nu$	Source
$\mathcal{B}(\%)$	3.58(5)(5)	0.309(12)(6)	CLEO-c Tag
$\mathcal{B}(\%)$	3.56(3)(11)	0.301(11)(10)	CLEO-c NoTag
$\mathcal{B}(\%)$	3.58(18)	0.360(60)	PDG04
$|f_+(0)|$	0.761(10)(7)	0.660(28)(11)	CLEO-c Tag
$|f_+(0)|$	0.749(5)(10)	0.636(17)(13)	CLEO-c NoTag
m_{pole} (GeV)	1.96(3)(1)	1.95(4)(2)	CLEO-c Tag
m_{pole} (GeV)	1.97(2)(1)	1.89(3)(1)	CLEO-c NoTag
α	0.22(5)(2)	0.17(10)(5)	CLEO-c Tag
α	0.21(4)(3)	0.32(7)(3)	CLEO-c Tag

FIG. 9: U distributions for (a) D^+ and (b) D^0 decays into $\rho e^+\nu$ candidates. The dashed curve shows the signal, the dotted curves show various backgrounds and the solid curve the sum.

TABLE III: Rare semileptonic decay branching fractions

Decay	$\mathcal{B} \times 10^{-4}$
$D^0 \to \rho^- e^+\nu$	$15.6 \pm 1.6 \pm 0.9$
$D^+ \to \rho^0 e^+\nu$	$23.2 \pm 2.0 \pm 1.2$
$D^+ \to \omega e^+\nu$	$14.9 \pm 2.7 \pm 0.5$
$D^+ \to \phi e^+\nu$	< 2 at 90% CL
$D^+ \to \eta e^+\nu$	$12.9 \pm 1.9 \pm 0.7$
$D^+ \to \eta' e^+\nu$	< 3 at 90% CL
$D^0 \to K^-\pi^+\pi^- e^+\nu$	$2.9^{+1.9}_{-1.0} \pm 0.5$

using both charge and neutral modes [22].

Other results on semileptonic decays from CLEO-c include measurement of the inclusive D^0 and D^+ semileptonic branching fractions of $(6.46 \pm 0.17 \pm 0.13)\%$, and $(16.13 \pm 0.20 \pm 0.33)\%$, respectively, leading to a measurement of the partial width ratio of $\Gamma(D^+)/\Gamma(D^0) = (0.985 \pm 0.028 \pm 0.015)$, consistent with isospin symmetry [26].

IV. CONCLUSIONS

CLEO-c measurements of leptonic and semileptonic decays have already reached precisions that provide very useful benchmarks for testing of QCD theories. From leptonic decays we have

$$
\begin{aligned}
f_{D^+} &= (222.6 \pm 16.7^{+2.8}_{-3.4}) \text{ MeV}, \qquad (12)\\
f_{D_s^+} &= (280.1 \pm 11.6 \pm 6.0) \text{ MeV},\\
f_{D_s^+}/f_{D^+} &= 1.26 \pm 0.11 \pm 0.03 .
\end{aligned}
$$

These results are consistent with most theoretical calculations including those of unquenched lattice QCD [20].

CLEO-c is also breaking new ground in the study of semileptonic decays. Form-factors in Cabibbo suppressed decays are reaching an unprecedented level of accuracy and are also confronting theory.

Acknowledgments

[1] G. Buchalla, A. J. Buras and M. E. Lautenbacher, Rev. Mod. Phys. **68**, 1125 (1996).
[2] A. Abulencia et al. (CDF), "Observation of $B_s\overline{B}_s$ Oscillations," [hep-ex/0609040]; see also V. Abazov et al. (D0), [hep-ex/0603029].
[3] C. Davies et al., Phys. Rev. Lett. **92**, 022001 (2004).
[4] M. Artuso et al. (CLEO), Phys. Rev. Lett. **95**, 251801 (2005);
[5] G. Bonvicini, et al. (CLEO) Phys. Rev. **D70**, 112004 (2004).
[6] D. Silverman and H. Yao, Phys. Rev. **D38**, 214 (1988).
[7] A. G. Akeroyd, Prog. Theor. Phys. **111**, 295 (2004); A. G. Akeroyd and C. H. Chen [hep-ph/0701078].
[8] J. Hewett, [hep-ph/9505246]; W.-S. Hou, Phys. Rev. **D48**, 2342 (1993).
[9] M. Chadha et al. (CLEO), Phys. Rev. **D58**, 032002 (1998).
[10] B. Aubert et al. (BaBar) [hep-ex/0607094].
[11] W.-M. Yao et al. (PDG), Journal of Physics **G 33**, 1 (2006)
[12] S. Stone, [hep-ph/0605134].
[13] S. Stone, [hep-ex/0610026].
[14] P. Rubin et al. (CLEO), Phys. Rev. **D73**, 112005 (2006).
[15] C. Aubin et al., Phys. Rev. Lett. **95**, 122002 (2005).
[16] T. W. Chiu et al., Phys. Lett. **B624**, 31 (2005).
[17] M. Artuso, "Status and future perspectives on V_{cs} and V_{cd}, Expermimental," presented at 4th Int. Workshop on the CKM Unitarity Triangle, Dec., 2006, Nagoya, Japan.
[18] T. Becher and R. J. Hill, Phys. Lett. **B633**, 61 (2006); R. J. Hill, [hep-ph/0606023].
[19] D. Becirevic and A. B. Kaidalov, Phys. Lett. **B478**, 417 (2000).
[20] See references to other theoretical predictions in [4].
[21] C. Aubin et al. , Phys. Rev. Lett., **95**, 122002 (2006).
[22] Y. Gao et al. (CLEO), presented at XXXIII Int. Conf. on High Energy Physics, Moscow, Russia, July, 2006.
[23] B. Grinstein and D. Pirjol, Phys. Rev. **D70**, 114005 (2004) [hep-ph/0404250].
[24] M. R. Shepherd et al. (CLEO), Phys. Rev. **D74**, 052001 (2006).
[25] J.M. Link et al. (FOCUS), Phys. Lett. **B 633**, 183 (2006).
[26] N. E. Adam et al. (CLEO), Phys. Rev. Lett. **97**, 251801 (2006).